

# On the Spatial Performance of Users in Indoor VLC Networks with Multiple Reflections

Abhishek K. Gupta and Adrish Banerjee

## Abstract

In this paper, we present a stochastic geometry based framework to analyze the performance of downlink indoor visible light communication (VLC) networks at a typical receiver while considering reflections from the walls. A typical receiver is a arbitrarily located user in the room and may not necessarily be at the center and hence sees an asymmetric transmitter location process and interference at itself. We first derive the signal-to-interference-plus-noise ratio (SINR) and rate coverage probability for a typical user. We then present a framework to model the impact of wall reflections and extend the analysis to study the performance of VLC network in the presence of wall reflections. We show that the impact of user's location and reflections is significant on the performance of the user.

## I. INTRODUCTION

Visible light communication is an attractive option to mitigate the problem of spectrum scarcity as demand for data services explode. One can achieve higher capacity, and more secure communication using VLC [1]–[3]. It allows significant power savings as visible light sources can serve the dual role of communications as well as room illumination. However, it suffers from high interference from other light sources, as well as significant blockage losses and hence it is especially suited for indoor communication applications [4].

Motivated by their potential, there has been recent push towards studying VLC networks [5]. In [6], authors analyzed the effect of transmitted power, dimming and node failure on the network coverage inside a horizontal plane in a room. In [7], authors studied the effect of field of view of receiver, effect of inter symbol interference and reflections on the performance of VLC system. They have shown that average power by including reflections is about 0.5 dB more than the direct received average power. Stochastic geometry has emerged as a tractable approach to analyze

The authors are with the department of Electrical Engineering at Indian Institute of Technology Kanpur, India 208016. Email IDs: gkrabhi@iitk.ac.in, adrish@iitk.ac.in.

wireless systems and it has been recently applied to analyze VLC networks in some early work [8]–[10]. In [8], authors have considered an optical orthogonal frequency division multiplexing (OFDM) based indoor attocell network and computed outage probability and achievable rates for different network deployments. In [9], authors have characterized the rate as well as coverage of different radio frequency (RF) and VLC co-existing systems under different configurations using stochastic geometry. The main limitation of above mentioned analytical works [8]–[10] is due to their assumption of stationarity of VLC network. Since VLC networks are confined in room boundaries, each user may not necessarily see similar serving transmitter’s distribution and interference field. Hence the user’s performance may depend on its location. This effect is more evident in the presence of wall reflections as these reflections may significantly affect corner users. Therefore, it is important to include the impact of users’ location in the performance analysis especially in the presence of wall reflections which is the main focus of this work.

The main contributions of the paper are as follows:

- We present a stochastic geometry based framework to analyze the performance of a downlink indoor VLC network at a typical arbitrarily located user in the room and may not necessarily be at the center. It is in general difficult to compute the distribution of the distance of the serving base-station (BS) from the user when the BSs process is non-stationary. We give a technique based on Campbell-Mecke theorem [11], which does not require this distribution computation. This technique is valid for SINR threshold greater than 1 which is typically the case. We then derive the SINR and rate coverage probability for a typical user.
- We present a model to include the impact of wall reflections and extend the analysis to study the performance in the presence of wall reflections.
- Finally, we provide some numerical results showing the impact of user’s location and reflections. We observe that users location significantly affect the performance of the network. In the presence of reflections, corner users are affected more due to increased non line-of-sight interference.

## II. SYSTEM MODEL

### *A. Network Model*

We consider an indoor downlink VLC network with optical attocells (OAs) operating at the same frequency band. We consider a room with height (desktop level to roof level)  $h$  and length and width  $2a$ . Without loss of generality, we can assume that center of the room is at the origin.

The 2D floor of the room is denoted by set  $\mathcal{S}(0, a)$  where  $\mathcal{S}(\mathbf{x}, a)$  denotes a square at center  $\mathbf{x}$  with sides of length  $2a$ . The locations of OAs are modeled as a 2-D homogeneous Poisson point process (PPP)  $\Phi = \{\mathbf{x}_i \in \mathbb{R}^2\}$  with a density of  $\lambda$  on the roof top in area  $\mathcal{S}(0, a)$ . Hence, the  $i$ th OA's location is given as  $(\mathbf{x}_i, h)$ . Each OA consists of LEDs oriented vertically downwards. The users are distributed as a homogeneous PPP at the desktop level with density  $\lambda_u$  across the room. A typical user (*i.e.* arbitrarily selected user) is located uniformly in the room. Let us denote the location of the typical user with  $(\mathbf{y}, 0)$ . Here,  $\mathbf{y} = (y_1, y_2) \in \mathbb{R}^2$  such that  $y_1, y_2 \sim U(-a, a)$ .

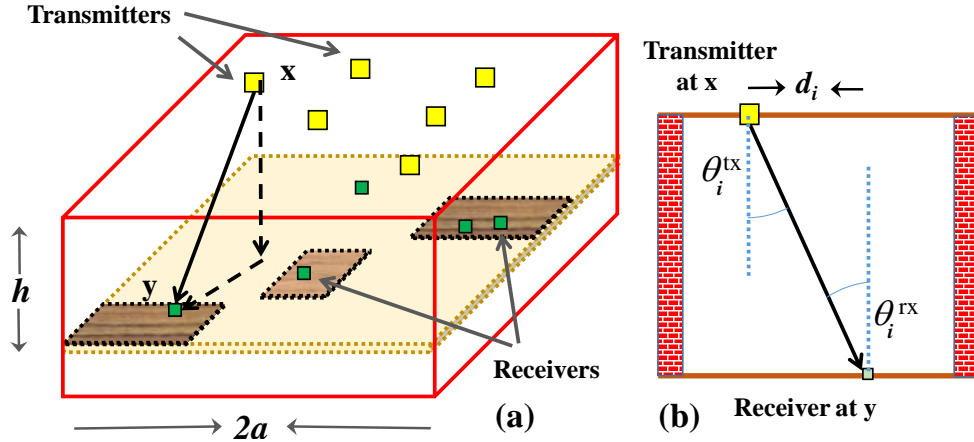


Fig. 1: Illustration showing (a) the transmitter (tx) and receiver (rx) locations (b) the propagation model between a tx-rx pair.

### B. Channel Model

We assume that the transmitters follow Lambertian emission radiation profile and they operate within the linear dynamic range of the current-to-power characteristic curve. The channel direct current gain between the user and  $i$ th OA can be modeled as follows [10]

$$G_i = (m + 1) \xi \frac{A_{pd}}{2\pi d_i^2} \cos^m(\theta_i^{\text{tx}}) \cos(\theta_i^{\text{rx}}) G_c(\theta_i^{\text{rx}}) G_f(\theta_i^{\text{rx}}) \quad (1)$$

where  $d_i$  is the distance of the user to  $i$ th OA.  $m$  denotes the order of Lambertian emission and is given as  $m = 1/\log_2(\sec \Psi_{\text{HALF}})$  where  $\Psi_{\text{HALF}}$  is the semi angle of transmitter's LEDs.  $\theta_i^{\text{tx}}$  and  $\theta_i^{\text{rx}}$  represent the  $i$ th OA's irradiance and incidence angle with respect to the user.  $A_{pd}$  denotes the detection area of the photodetector (PD) at the receiver.  $G_f(\theta_i^{\text{rx}})$  and  $G_c(\theta_i^{\text{rx}})$  are the

gains of the receivers optical filter and concentrator and assumed to be constant.  $\xi$  denotes the average responsivity of PD. From Fig. 1(b), we can observe that

$$\cos(\theta_i^{\text{tx}}) = \cos(\theta_i^{\text{rx}}) = h/\sqrt{h^2 + d_i^2}. \quad (2)$$

Substituting values of  $\cos(\theta_i^{\text{tx}})$  and  $\cos(\theta_i^{\text{rx}})$  into (1), we get

$$G_i = \alpha(|\mathbf{x}_i - \mathbf{y}|^2 + h^2)^{-\beta/2}$$

where  $\alpha = (m + 1)A_{pd}\xi G_f G_c h^{m+1}/(2\pi)$  and  $\beta = m + 3$ . The transmit power of OA is assumed to be  $P_{\text{tx}}$ . We assume direct current OFDM as modulation scheme [10]. Hence, the receiver power from the  $i$ th transmitter is given as

$$P_i = P_{\text{tx}}\alpha^2\ell(\mathbf{x}, \mathbf{y}). \quad (3)$$

where  $\ell(\mathbf{x}, \mathbf{y})$  be defined as  $\ell(\mathbf{x}, \mathbf{y}) = (|\mathbf{x} - \mathbf{y}|^2 + h^2)^{-\beta}$ .

### C. Association and SINR model

If the considered user is associated with  $i$ th OA located at  $\mathbf{x}_i$ , the SINR at this user is given as

$$\text{SINR}_i(\mathbf{y}) = \frac{\ell(\mathbf{x}_i, \mathbf{y})}{I(\Phi \setminus \mathbf{x}_i) + \sigma^2} \quad (4)$$

where  $I$  denotes the sum interference and given as

$$I(\Phi \setminus \mathbf{x}_i) = \sum_{\mathbf{x}_j \in \Phi \setminus \mathbf{x}_i} \ell(\mathbf{x}_j, \mathbf{y}). \quad (5)$$

Here,  $\sigma^2$  is effective noise and given as  $\sigma^2 = N_0 B_f / (\alpha^2 P_{\text{tx}})$  with  $N_0$  being the noise power spectral density and  $B_f$  being the user bandwidth. We consider maximum received signal power-based association criterion which is equivalent to the nearest BS association criterion due to lack of random fading in the VLC environment. Suppose that the associated BS's index is 0, then  $\mathbf{x}_0 = \arg \max_{\mathbf{x}_i} \ell(\mathbf{x}_i, \mathbf{y})$ . The SINR at this user is equal to  $\text{SINR}_0(\mathbf{y})$ . In the next sections, we will present analytical framework to compute performance of this typical user. We will first consider VLC networks without any reflections in the Section III. We then present a framework to model reflections in VLC network in the Section IV and extend the analysis to study their impact.

### III. ANALYSIS OF SINR AND RATE COVERAGE

In this section, we will first compute the probability of SINR and rate coverage of a user at  $\mathbf{y}$  and then compute the coverage for a typical user in a VLC network without any reflections.

#### A. SINR Coverage Probability

The SINR coverage probability  $P_c(\tau, \mathbf{y})$  of a user located at  $\mathbf{y}$  is defined as the probability that the SINR at this user is greater than the threshold  $\tau$  *i.e.*

$$P_c(\tau, \mathbf{y}) = \mathbb{P}[\text{SINR}_0(\mathbf{y}) > \tau]. \quad (6)$$

We assume that SINR threshold  $\tau \geq 1$ . From [12], it can be shown that at maximum, only one OA can have SINR greater than 1 (and hence  $\tau$ ). In other words,

$$\mathbb{1}(\text{SINR}_0(\mathbf{y}) > \tau) = \sum_{\mathbf{x}_i \in \Phi} \mathbb{1}(\text{SINR}_i(\mathbf{y}) > \tau).$$

Therefore, the probability of SINR coverage is given as

$$P_c(\tau, \mathbf{y}) = \mathbb{E} \left[ \sum_{\mathbf{x}_i \in \Phi} \mathbb{1}(\text{SINR}_i(\mathbf{y}) > \tau) \right]. \quad (7)$$

From Campbell-Mecke theorem and Sliynak theorem [11], (7) can be further solved as

$$\begin{aligned} P_c(\tau, \mathbf{y}) &= \lambda \int_{\mathcal{S}(0,a)} \mathbb{P} \left[ \frac{\ell(\mathbf{x}, \mathbf{y})}{I(\Phi) + \sigma^2} > \tau \right] d\mathbf{x} \\ &= \lambda \int_{\mathcal{S}(0,a)} \mathbb{P} \left[ I < \tau^{-1} (|\mathbf{x} - \mathbf{y}|^2 + h^2)^{-\beta} - \sigma^2 \right] d\mathbf{x} \\ &= \lambda \int_{\mathcal{S}(-\mathbf{y},a)} \mathbb{P} \left[ I < \tau^{-1} (|\mathbf{x}|^2 + h^2)^{-\beta} - \sigma^2 \right] d\mathbf{x}. \end{aligned} \quad (8)$$

where the last step is due to the transformation  $\mathbf{x} \rightarrow \mathbf{x} + \mathbf{y}$ . Note that  $\mathbb{P}[I < s]$  is non zero only when  $s > 0$  which is equivalent to  $\{\mathbf{x} : |\mathbf{x}| < a_D \triangleq [\tau^{-1/\beta} \sigma^{-2/\beta} - h^2]^{1/2}\}$ . Now, (8) can be written as

$$P_c(\tau, \mathbf{y}) = \lambda \int_{A_{\mathbf{y}}} \mathbb{P} \left[ I < \tau^{-1} (|\mathbf{x}|^2 + h^2)^{-\beta} - \sigma^2 \right] d\mathbf{x} \quad (9)$$

where  $A_{\mathbf{y}} = \mathcal{S}(-\mathbf{y}, a) \cap \mathcal{B}(0, a_D)$ . Here,  $\mathcal{B}(\mathbf{a}, r)$  denotes a ball of radius  $r$  and center  $\mathbf{a}$ . Note that due to absence of fading, there is a certain radius  $a_D$  around the receiver in which associated OA must be located otherwise the signal strength is smaller than the noise power, making SNR

(and hence SINR) less than  $\tau$ . From the Gill Pelaez inversion Lemma [13], the CDF of the sum interference  $I$  can be expressed in terms of its Laplace transform  $\mathcal{L}_I()$  as

$$\mathbb{P}[I < s] = \frac{1}{2} - \frac{1}{\pi} \int_0^\infty \frac{1}{t} \text{Im} [e^{-jts} \mathcal{L}_I(-jt)] dt. \quad (10)$$

From (9) and (10), the SINR coverage probability is

$$P_c(\tau, \mathbf{y}) = \lambda \int_{\mathcal{A}(\mathbf{y})} \left[ \frac{1}{2} - \frac{1}{\pi} \int_0^\infty \frac{1}{t} \text{Im} \left[ e^{-jt(\tau^{-1}(|\mathbf{x}|^2 + h^2))^{-\beta} - \sigma^2} \mathcal{L}_I(-jt) \right] dt \right] d\mathbf{x}. \quad (11)$$

Note that (11) requires computation of  $\mathcal{L}_I()$  which we give in the following Lemma.

**Lemma 1.** *The Laplace transform of the sum interference at a receiver at location  $\mathbf{y}$  is given as  $\mathcal{L}_I(s) =$*

$$\exp \left( -\lambda \int_{\mathcal{S}(-\mathbf{y}, a)} \left( 1 - \exp \left[ \frac{-s}{(|z|^2 + h^2)^\beta} \right] \right) dz \right). \quad (12)$$

*Proof:* See Appendix A; ■

Using Lemma 1 and (11), we get the following theorem.

**Theorem 1.** *The probability of SINR coverage of a receiver located at location  $\mathbf{y}$  in a indoor VLC network is given as*

$$P_c(\tau, \mathbf{y}) = \frac{\lambda |\mathbf{A}_\mathbf{y}|}{2} - \frac{\lambda}{\pi} \int_0^\infty \frac{1}{t} \text{Im} \left[ e^{jt\sigma^2} \mathcal{F}(jt\tau^{-1}, \mathbf{A}_\mathbf{y}) \mathcal{K}(jt, \mathcal{S}(-\mathbf{y}, a)) \right] dt \quad (13)$$

where  $\mathcal{F}(\cdot)$  and  $\mathcal{K}(\cdot)$  are given as

$$\begin{aligned} \mathcal{F}(s, \mathbf{A}) &= \int_{\mathbf{A}} e^{-s(|\mathbf{x}|^2 + h^2)^{-\beta}} d\mathbf{x} \\ \mathcal{K}(s, \mathbf{A}) &= \exp \left( -\lambda \int_{\mathbf{A}} \left( 1 - \exp \left[ \frac{s}{(|z|^2 + h^2)^\beta} \right] \right) dz \right). \end{aligned}$$

*Proof:* See Appendix B. ■

From Theorem 1, the following corollaries establishing the relation between performance of a corner (located at  $[a, a]$ ) and a center (located at  $[0, 0]$ ) user can be derived:

**Corollary 1.** *The SINR coverage for a corner user in a VLC network with  $\lambda$  density of OAs and room size  $2a$  is equal to that of a center user in another VLC network with similar parameters but with  $\lambda/4$  density of the OAs and  $4a$  room size.*

**Corollary 2.** *For the case with no noise, the SINR coverage for a corner user in a room of height  $h$  is equal to that of a center user in a room of height  $\frac{h}{2}$ .*

**Corollary 3.** *For the case where noise is zero and the transmitters and the receivers are at the same height, the SINR coverage for a corner user is equal to that of a center user.*

Now, the SINR coverage probability for the arbitrarily located typical user can be computed as

$$\begin{aligned} P_c(\tau) &= \mathbb{P}[\text{SINR}_0 > \tau] \\ &\stackrel{(a)}{=} \frac{\int_{\mathcal{S}(0,a)} P_c(\tau, \mathbf{y}) d\mathbf{y}}{|\mathcal{S}(0,a)|} = \frac{1}{4a^2} \int_{\mathcal{S}(0,a)} P_c(\tau, \mathbf{y}) d\mathbf{y} \end{aligned} \quad (14)$$

where (a) is due to the uniform distribution assumption of  $\mathbf{y}$ .

### B. Rate Coverage

In this section, we derive the rate coverage which is defined as the probability that the rate of a user at  $\mathbf{y}$  is greater than the threshold  $\rho$ ,

$$R_c(\rho, \mathbf{y}) = \mathbb{P}[\text{Rate}_0(\mathbf{y}) > \rho]. \quad (15)$$

Let  $W$  be the total bandwidth available at each OA. Assuming the time-division access for providing access to multiple users at a single OA [8], the per user rate can be given as [9]

$$\text{Rate} = \zeta_1 \frac{W}{n} \log(1 + \zeta_2 \text{SINR}). \quad (16)$$

where  $n$  is the mean number of users (or load) associated with the serving OA and  $\zeta_1, \zeta_2$  are some coefficients due to practical constraints. Since the user distribution is also assumed to be PPP, the mean load with the typical user can be modeled similarly to [14] to be  $n = 1 + 1.28\lambda_u/\lambda$ . Now,  $R_c(\rho, \mathbf{y})$  can be derived in terms of coverage probability as follows:

$$\begin{aligned} R_c(\rho, \mathbf{y}) &= \mathbb{P}[\text{Rate}(\mathbf{y}) > \rho] \\ &= \mathbb{P}\left[\frac{W\zeta_1}{n} \log(1 + \zeta_2 \text{SINR}(\mathbf{y})) > \rho\right] \\ &= \mathbb{P}\left[\text{SINR} > \zeta_2^{-1}(2^{\rho \frac{n}{W\zeta_1}} - 1)\right] = P_c(\zeta_2^{-1}(2^{\rho n/(W\zeta_1)} - 1), \mathbf{y}) \end{aligned}$$

where  $P_c$  is given in (13). The rate coverage for an arbitrarily located typical user is given as

$$R_c(\rho) = P_c\left(\zeta_2 \left(2^{\zeta_1^{-1}\rho n/W} - 1\right)\right). \quad (17)$$

#### IV. COVERAGE ANALYSIS WITH REFLECTIONS

##### A. Modeling Reflections

Reflections can be modeled using image of the original transmitters with respect to the walls (See Fig. 2(a)) [15]. Let us first consider single reflections. For a given Tx-Rx pair, there are total 4 reflection images formed on the other side of walls (See Fig. 2(b)). The first reflection images of transmitters (let us call them virtual transmitters) form a PPP  $\Phi_1$  with density  $\lambda$  in the area  $F_I = \mathcal{S}(0, a) \oplus 2aG_1$  (See vertically shaded area in Fig. 2(c)) where  $G_1 = \{(\pm 1, 0), (0, \pm 1)\}$  and  $\oplus$  denotes the Minkowski sum of two sets. The received power at the user  $\mathbf{y}$  from a virtual transmitter located at  $\mathbf{x}$  is given as (See Fig. 2(a))

$$\ell(\mathbf{x}, \mathbf{y}) = \eta(|\mathbf{x} - \mathbf{y}|^2 + h^2)^{-\beta}, \quad \mathbf{x} \in F_I \quad (18)$$

where  $\eta$  is due to reflection loss and dependent on the wall material [16]. Combining the pathloss for  $\mathbf{x} \in \mathcal{S}(0, a)$  (given in (3)) and  $\mathbf{x} \in F_I$  (given in (18)), we get the following pathloss function

$$\ell(\mathbf{x}, \mathbf{y}) = \begin{cases} (|\mathbf{x} - \mathbf{y}|^2 + h^2)^{-\beta}, & \mathbf{x} \in \mathcal{S}(0, a) \\ \eta(|\mathbf{x} - \mathbf{y}|^2 + h^2)^{-\beta}, & \mathbf{x} \in F_I \end{cases}.$$

Similarly second reflection images of transmitters (also virtual transmitters) form a PPP  $\Phi_2$  with density  $\lambda$  in the area  $F_{II} = \mathcal{S}(0, a) \oplus 4aG_2$  (See horizontally shaded area in Fig. 2(c)) where  $G_2 = \{(0, \pm 1), (\pm 1, 0), (\pm \frac{1}{2}, \pm \frac{1}{2})\}$  with reflection loss coefficient  $\eta^2$ . In general,  $k$ th reflection images of transmitters form a PPP  $\Phi_k$  in the area  $F_k = \mathcal{S}(0, a) \oplus 2kaG_k$  with reflection loss coefficient as  $\eta^k$  where  $G_k = \{(\pm \frac{k_1}{k}, \pm \frac{k_2}{k}) : k_1 + k_2 = k, k_1 \in \mathbb{N}\}$ . Note that the cardinality of  $G_k$  is  $|G_k| = 4k$  (for  $k > 0$ ). Let us define  $G_0 = \{(0, 0)\}$  and  $F_0 = \mathcal{S}(0, a)$  for completeness. Hence, the aggregate pathloss function considering all transmitters (real and virtual) is given as

$$\ell(\mathbf{x}, \mathbf{y}) = \begin{cases} (|\mathbf{x} - \mathbf{y}|^2 + h^2)^{-\beta}, & \text{if } \mathbf{x} \in \mathcal{S}(0, a) \\ \eta^k (|\mathbf{x} - \mathbf{y}|^2 + h^2)^{-\beta}, & \text{if } \mathbf{x} \in \mathcal{S}(0, a) \oplus 2akG_k. \end{cases} \quad (19)$$

Note that all sets  $F_k$  are mutually disjoint and cover whole space  $\mathbb{R}^2$ . We have assumed their independence. Therefore, the union of all reflection images and real transmitters form a PPP with density  $\lambda$  due to the superposition theorem [12].



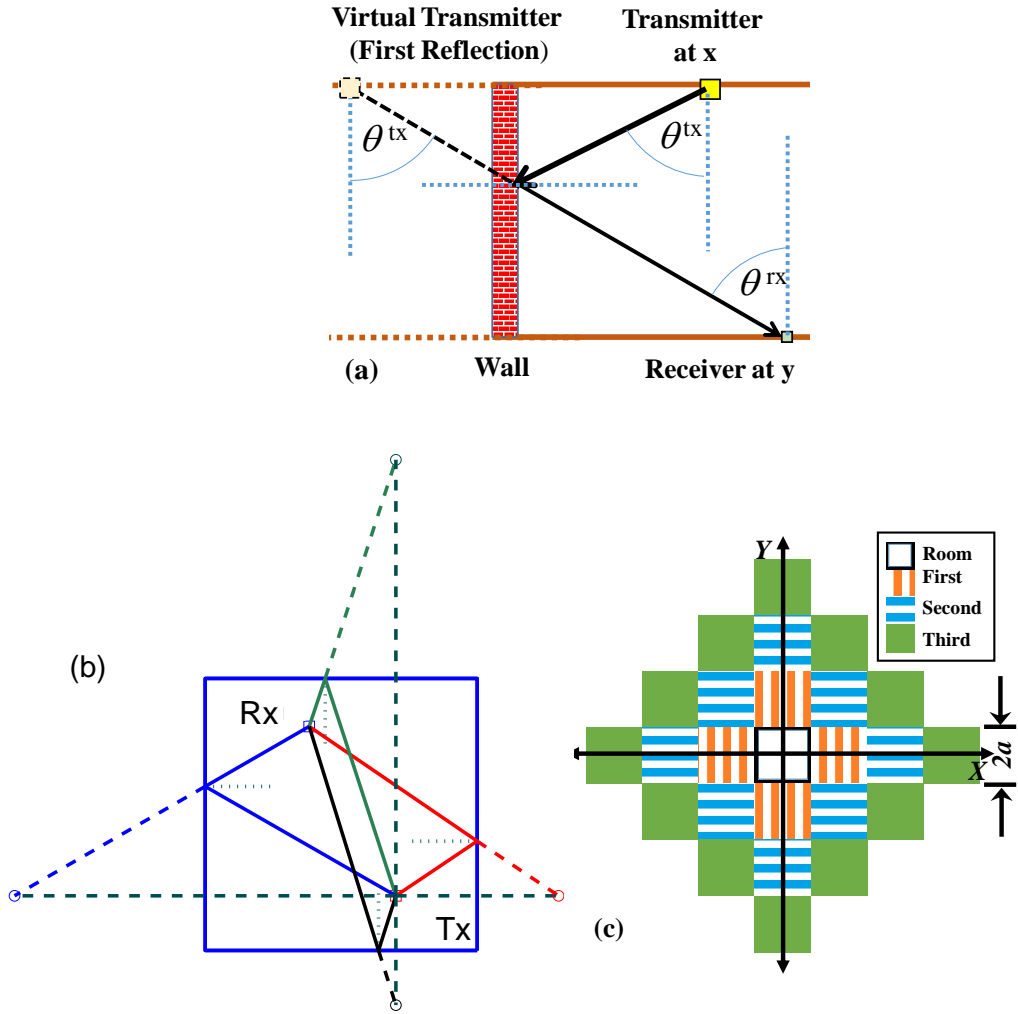


Fig. 2: (a) The reflection of a signal from a transmitter  $x$  for the receiver  $y$  (YZ plane) (b) The four reflection images (first order) of  $x$  as seen by  $y$  (XY plane) (c) Illustration showing the locations of reflection images up to the third order reflections.

### B. SINR Coverage

Let us consider reflections upto the  $K$ th order only. In this case, the union of all transmitters will be a PPP over the space  $\cup_k F_k$ . Now, similar to the no reflection case, we can apply Campbell-

Mecke theorem and Sliynak theorem in (7) to get

$$\begin{aligned}
P_c(\tau, \mathbf{y}) &= \lambda \sum_{k=0}^K \int_{F_k(0,a)} \mathbb{P} \left[ \frac{\ell(\mathbf{x}, \mathbf{y})}{I(\Phi) + \sigma^2} > \tau \right] d\mathbf{x} \\
&= \lambda \sum_{k=0}^K \int_{F_k(0,a)} \mathbb{P} \left[ I < \tau^{-1} \eta^k (|\mathbf{x} - \mathbf{y}|^2 + h^2)^{-\beta} - \sigma^2 \right] d\mathbf{x} \\
&= \lambda \sum_{k=0}^K \int_{F_k(-\mathbf{y},a)} \mathbb{P} \left[ I < \tau^{-1} \eta^k (|\mathbf{x}|^2 + h^2)^{-\beta} - \sigma^2 \right] d\mathbf{x} \tag{20}
\end{aligned}$$

where  $F_k(-\mathbf{y}, a)$  is the translation of the set  $F_k(0, a)$  by the vector  $\mathbf{y}$ . Note that  $\mathbb{P}[I < \cdot]$  is non-zero only for  $\{\mathbf{x} : |\mathbf{x}| < b_D^k \triangleq \left[ \eta^{k/\beta} (\tau \sigma^2)^{-1/\beta} - h^2 \right]^{1/2}\}$ . Hence, (20) is written as

$$P_c(\tau, \mathbf{y}) = \lambda \sum_{k=0}^K \int_{B_{k\mathbf{y}}} \mathbb{P} \left[ I < \eta^k \tau^{-1} (|\mathbf{x}|^2 + h^2)^{-\beta} - \sigma^2 \right] d\mathbf{x}$$

where  $B_{k\mathbf{y}} = F_k(-\mathbf{y}, a) \cap \mathcal{B}(0, b_D^k)$ . Here,  $b_D^k$  shows the radius in which virtual transmitter of  $k$ th order must be located. Now, following the steps similar to Appendix A, we can compute the Laplace transform of interference which is given in the following Lemma.

**Lemma 2.** *The Laplace transform of the sum interference at a receiver at location  $\mathbf{y}$  is given as*

$$\mathcal{L}_I(s) = \exp \left( -\lambda \sum_{k=0}^{\infty} \int_{F_k(-\mathbf{y},a)} \left( 1 - \exp \left[ \frac{-s\eta^k}{(|\mathbf{z}|^2 + h^2)^\beta} \right] \right) d\mathbf{z} \right)$$

where (21)

$$F_k(\mathbf{z}, a) = \mathcal{S}(\mathbf{z}, a) \oplus 2kaG_k. \tag{22}$$

Using Lemma 1 and the Gil-Paleaz Lemma similar to the previous section, we get the following theorem.

**Theorem 2 (Multiple Reflections).** *The probability of SINR coverage of a receiver located at location  $\mathbf{y}$  in a indoor VLC network with maximum  $K$ th order reflections is given as*

$$P_c(\tau, \mathbf{y}) = \frac{\lambda |\mathbf{B}_{\mathbf{y}}|}{2} - \frac{\lambda}{\pi} \int_0^\infty \frac{1}{t} \text{Im} \left[ e^{jt\sigma^2} \mathcal{F}_M(jt/\tau, \mathbf{y}) \mathcal{K}_M(jt, \mathbf{y}) \right] dt \tag{23}$$

where  $\mathcal{F}_M(\cdot)$  and  $\mathcal{K}_M(\cdot)$  are given as

$$\begin{aligned}
\mathcal{F}_M(s, \mathbf{z}) &= \sum_{k=0}^K \int_{B_{k\mathbf{z}}} e^{-s\eta^k (|\mathbf{x}|^2 + h^2)^{-\beta}} d\mathbf{x} \\
\mathcal{K}_M(s, \mathbf{z}) &= \exp \left( -\lambda \sum_{k=0}^K \int_{F_k(-\mathbf{z},a)} \left( 1 - e^{-\frac{s\eta^k}{(|\mathbf{z}|^2 + h^2)^\beta}} \right) d\mathbf{z} \right)
\end{aligned}$$

$$\text{with } \mathcal{B}_{\mathbf{y}} = \cup_{k=0}^{\infty} (\mathcal{F}_k(-\mathbf{y}, a) \cap \mathcal{B}(0, b_D^k)).$$

Following the steps similar to the Section III, SINR and rate coverage for an arbitrarily located user can be computed.

TABLE I: Numerical values for parameters

Params	Value	Params	Value	Params	Value
$\Psi_{\text{HALF}}$	$60^\circ$	$m$	1	$N_0 B_f$	-117dBm
$A_{pd}$	$.01 \text{ m}^2$	$\xi$	0.4 A/W	$G_f, G_c$	1,2.25
$P_{tx}$	30 dBm	$a$	9 m	$h$	3.5 m
$W$	1GHz	$(\lambda, \lambda_u)$	$(.1, .5)/\text{m}^2$	$\zeta_1, \zeta_2$	(1,1)

## V. NUMERICAL RESULTS

We will now provide some numerical results based on the analysis and derive design insights for VLC networks. In the simulation, we have considered a indoor VLC network deployed in a room with dimensions  $18 \times 18 \times 3.5 \text{ m}^3$ . All relevant simulation parameters are given in the Table I [10].

**SINR and rate coverage of users at various locations:** We have considered four different user locations: user located at the corner ( $L_1 = [a, a]$ ), the edge ( $L_2 = [a, 0]$ ), halfway ( $L_3 = [\frac{a}{\sqrt{2}}, \frac{a}{\sqrt{2}}]$ ) and the center ( $L_4 = [0, 0]$ ) of the room. Fig. 3 and Fig. 4 show the SINR and rate coverage of the users at the above mentioned locations for no reflection case. We can observe that the performance of a VLC network significantly depends on the user location. Hence, the typical user can not be assumed to be at the center only and it is very important to include the impact of user's location into its performance. This effect is due to the non-zero value of room height ( $h$ ) as discussed in the Section III.

**SINR coverage of the typical user:** Motivated by the above mentioned result, we also show the SINR of a typical user (according to (14)) in Fig. 3. We can observe that the performance of a typical user can be approximated by the performance of a halfway user in the considered scenario.

**Impact of reflections:** We show the impact of the reflections with the help of an example of single order reflection with  $\eta = 0.07$ . Fig. 4 shows the rate coverage of the users at the above mentioned locations for no reflection case and reflection case. We can observe that median rate of the corner user decreased by 25% due to presence of reflections even when only single order

reflections are considered. This is due to the fact that reflection images rarely act as serving OAs but they add significantly to the sum interference. We can also see that rate coverage of center and halfway users are not impacted significantly when reflections are considered.

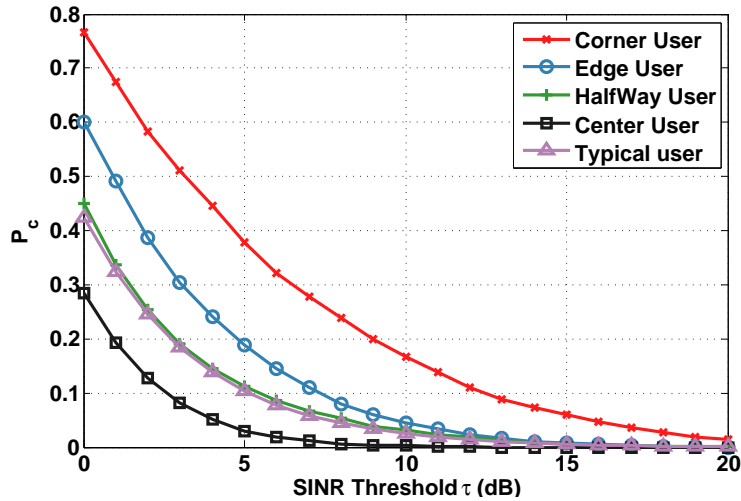


Fig. 3: Probability of SINR coverage for four user locations. Location of the users plays an important role in their performance.

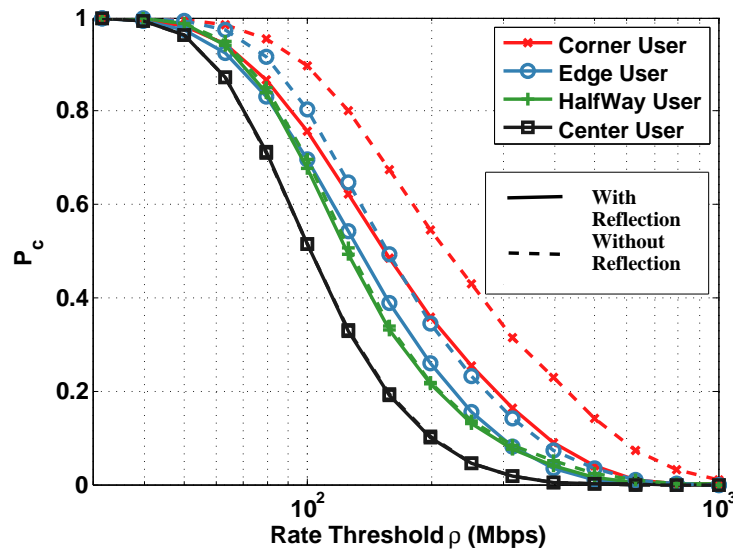


Fig. 4: Impact of reflections on the rate coverage. Corner and edge users are the ones facing the most degradation in their performance.

## VI. CONCLUSIONS

In this paper, we have presented a framework to analyze an indoor VLC network for a typical user while considering multiple reflections from the walls. We showed that SINR and rate coverage of a user significantly depend on the location of the user. We also showed that reflections can be an important factor while computing performance for corner and edge users.

### APPENDIX A

#### PROOF OF LEMMA 1

The Laplace transform of the sum interference is given as

$$\begin{aligned}\mathcal{L}_I(s) &= \mathbb{E} [e^{-sI}] = \mathbb{E} \left[ e^{-s \sum_{\mathbf{x}_i \in \Phi} \ell(\mathbf{x}, \mathbf{y})} \right] \\ &\stackrel{(a)}{=} \exp \left( -\lambda \int_{\mathcal{S}(0, a)} (1 - e^{-s\ell(\mathbf{x}, \mathbf{y})}) d\mathbf{x} \right) \\ &\stackrel{(b)}{=} \exp \left( -\lambda \int_{\mathcal{S}(-\mathbf{y}, a)} (1 - e^{-s\ell(\mathbf{x}, 0)}) d\mathbf{x} \right).\end{aligned}$$

Here (a) is due to PGFL of PPP [12] and (b) is due to the transformation  $\mathbf{x} \rightarrow \mathbf{x} + \mathbf{y}$ .

### APPENDIX B

#### PROOF OF THEOREM 1

From Lemma 1 and (11), the SINR coverage is given as

$$\begin{aligned}P_c(\tau, \mathbf{y}) &= \frac{\lambda |A_{\mathbf{y}}|}{2} - \frac{\lambda}{\pi} \int_{A_{\mathbf{y}}} \int_0^\infty \frac{1}{t} \text{Im} \left[ e^{-jt(\tau^{-1}(|\mathbf{x}|^2 + h^2)^{-\beta} - \sigma^2)} \right. \\ &\quad \left. \exp \left( -\lambda \int_{\mathcal{S}(-\mathbf{y}, a)} \left( 1 - \exp \left[ \frac{jt}{(|\mathbf{z}|^2 + h^2)^\beta} \right] \right) d\mathbf{z} \right) \right] dt d\mathbf{x}\end{aligned}$$

Now, expectation with respect to  $\mathbf{x}$  can be moved inside to get  $P_c(\tau, \mathbf{y})$

$$\begin{aligned}&= \frac{\lambda |A_{\mathbf{y}}|}{2} - \frac{\lambda}{\pi} \int_0^\infty \frac{1}{t} \text{Im} \left[ \int_{A_{\mathbf{y}}} e^{-jt(\tau^{-1}(|\mathbf{x}|^2 + h^2)^{-\beta} - \sigma^2)} d\mathbf{x} \right. \\ &\quad \left. \exp \left( -\lambda \int_{\mathcal{S}(-\mathbf{y}, a)} \left( 1 - \exp \left[ \frac{jt}{(|\mathbf{z}|^2 + h^2)^\beta} \right] \right) d\mathbf{z} \right) \right] dt.\end{aligned}$$

Now using taking noise term outside integration and applying the definition of  $\mathcal{K}$  and  $\mathcal{F}$ , we get the Theorem.

## REFERENCES

- [1] L. Feng, R. Q. Hu, J. Wang, P. Xu, and Y. Qian, "Applying VLC in 5G networks: Architectures and key technologies," *IEEE Network*, vol. 30, no. 6, pp. 77–83, Nov. 2016.
- [2] A. Jovicic, J. Li, and T. Richardson, "Visible light communication: opportunities, challenges and the path to market," *IEEE Commun. Mag.*, vol. 51, no. 12, pp. 26–32, Dec. 2013.
- [3] D. Karunatilaka, F. Zafar, V. Kalavally, and R. Parthiban, "LED based indoor visible light communications: state of the art," *IEEE Commun. Surveys & Tut.*, vol. 17, no. 3, pp. 1649–1678, 2015.
- [4] H. Elgala, R. Mesleh, and H. Haas, "Indoor optical wireless communication: Potential and state-of-the-art," *IEEE Commun. Mag.*, vol. 49, no. 9, pp. 56–62, Sep. 2011.
- [5] P. H. Pathak, X. Feng, P. Hu, and P. Mohapatra, "Visible light communication, networking, and sensing: A survey, potential and challenges," *IEEE Commun. Surveys Tut.*, vol. 17, no. 4, pp. 2047–2077, Fourthquarter 2015.
- [6] A. Vavoulas, H. G. Sandalidis, T. A. Tsiftsis, and N. Vaiopoulos, "Coverage aspects of indoor VLC networks," *Journal of Lightwave Technology*, vol. 33, no. 23, pp. 4915–4921, 2015.
- [7] T. Komine and M. Nakagawa, "Fundamental analysis for visible light communication system using LED lights," *IEEE Trans. Consumer Electronics*, vol. 50, no. 1, pp. 100–107, Feb. 2004.
- [8] C. Chen, D. A. Basnayaka, and H. Haas, "Downlink performance of optical attocell networks," *Journal of Lightwave Technology*, vol. 34, no. 1, pp. 137–156, Jan 2016.
- [9] H. Tabassum and E. Hossain, "Coverage and rate analysis for co-existing RF/VLC downlink cellular networks," *ArXiv:preprint:1710.01272*, Oct 2017.
- [10] L. Yin and H. Haas, "Coverage analysis of multiuser visible light communication networks," *IEEE Trans. Wireless Commun.*, vol. PP, no. 99, pp. 1–1, 2017.
- [11] F. Baccelli and B. Błaszczyszyn, *Stochastic Geometry and Wireless Networks*, 2nd ed. NOW Publishers, 2009, vol. 1.
- [12] J. G. Andrews, A. K. Gupta, and H. S. Dhillon, "A primer on cellular network analysis using stochastic geometry," *arXiv preprint arXiv:1604.03183*, 2016.
- [13] J. Gil-Pelaez, "Note on the inversion theorem," *Biometrika*, vol. 38, no. 3-4, pp. 481–482, 1951.
- [14] S. Singh, H. S. Dhillon, and J. G. Andrews, "Offloading in heterogeneous networks: modeling, analysis and design insights," *IEEE Trans. Wireless Commun.*, vol. 12, no. 5, pp. 2484 – 2497, May 2013.
- [15] K. Venugopal and R. W. Heath, "Millimeter wave networked wearables in dense indoor environments," *IEEE Access*, vol. 4, pp. 1205–1221, 2016.
- [16] W. J. Smith, *Modern Optical Engineering*, 4th ed. McGraw Hill Education, 2007.